Histol Histopathol (2023) 38: 1381-1390

Histology and Histopathology
From Cell Biology to Tissue Engineering

ORIGINAL ARTICLE Open Access

# Transcription factor ZNF488 accelerates cervical cancer progression through regulating the MEK/ERK signaling pathway

**Kena Weng, Lu Li and Haiping Zhou**

Department of Obstetrics and Gynecology, The Affiliated People's Hospital of Ningbo University, Ningbo, China

**Summary.** Cervical cancer (CC) is one of the most common gynecological malignancies worldwide. Zinc Finger Protein 488 (ZNF488) has been identified as an oncogene in nasopharyngeal carcinoma. However, its biological role and potential mechanism in CC remain to be elucidated. In the present study, upregulation of ZNF488 expression in human CC tissues was found in clinical samples and analyzed in The Cancer Genome Atlas (TCGA) dataset, which was associated with clinical staging and lymph node metastasis. Quantitative real time polymerase chain reaction (PCR) and western blot assays indicated that the expression of ZNF488 was up-regulated in CC cells. Cell colony formation and cell cycle analysis assays suggested that ZNF488 promoted CC cell proliferation and cycle progression. Knockdown of ZNF488 inhibited tumor growth of xenograft tumor mice *in vivo*, in agreement with the levels of ZNF488 and Ki-67. Moreover, transwell and western assays demonstrated that ZNF488 enhanced CC cell migration and invasion. Additionally, knockdown of ZNF488 also inhibited lung metastasis of CC cells *in vivo*. Further mechanism analysis implied that ZNF488 promoted the MEK/ERK signaling pathway. ERK inhibitor PD98059 significantly weakened the proliferation and epithelial-mesenchymal transformation (EMT) promotion effect of ZNF488. Collectively, ZNF488 exerts its oncogene function partially through modulating MEK/ERK signaling pathway in CC, indicating that ZNF488 may provide a promising therapeutic target for the treatment of CC.

**Key words:** ZNF488, Cervical cancer, Proliferation, Migration, Invasion, MEK/ERK

*Corresponding Author:* Kena Weng, Department of Obstetrics and Gynecology, The Affiliated People's Hospital of Ningbo University, 247 Renmin Road, Jiangbei District, Ningbo City, Zhejiang Province, 315000, China. e-mail: Wengkena123@163.com

www.hh.um.es. DOI: 10.14670/HH-18-568

## Introduction

Cervical cancer (CC) is one of the most common causes of tumors in women worldwide and is the leading cause of cancer death in women, especially in developing countries (Denny, 2012; Crosbie et al., 2013; Small et al., 2017; Canfell, 2019). Currently, high-risk human papillomavirus (HPV) infection is the key to the progression of cervical cancer (de Sanjose et al., 2010; Pal and Kundu, 2020). In addition, genetic alterations and epigenetic modifications also play important roles in regulating the occurrence and development of cervical cancer (de Sanjose et al., 2010; Hu et al., 2010; Nahand et al., 2020; Hashemipour et al., 2021; Rahimian et al., 2021; Razavi et al., 2021). At the same time, the main treatment methods for cervical cancer include surgery, radiotherapy and adjuvant chemotherapy, which significantly improve the survival rate of patients with cervical cancer (Denny, 2012; Stevanović et al., 2015). Unfortunately, more and more studies have shown that excessive drug resistance to radiotherapy or chemotherapy, recurrent recurrence and tumor metastasis limit the therapeutic effect, while the molecular mechanism that reveals the growth of cervical cancer has not been fully studied and understood. Therefore, there is an urgent need to find new or key therapeutic targets in order to develop effective and reliable therapeutic treatments.

Zinc finger protein was first discovered in 1983 in the transcription factor TFIIIA of *Xenopus laevis* oocytes, and is the most widely distributed protein class in the eukaryotic genome (Miller et al., 1985). It is possible that nearly 1% of human genome sequences encode proteins containing zinc finger structure (Hoovers et al., 1992). Zinc finger proteins play important roles in gene expression regulation, cell differentiation, embryo development, differentiation and maturation (Cassandri et al., 2017; Nagaoka and Sugiura, 2000). Zinc finger protein 488 (ZNF488) gene is located at 10q11.22, and the encoding protein consists of 340 amino acids with a molecular weight of about 38

kDa. It is a Kruppel C2H2 type zinc finger protein located in the nucleus, and its transcriptional regulation role is complex (Wang et al., 2006). ZNF488 has been reported to interact with a highly conserved oligodendrocyte specific transcription factor to participate in myelin regeneration and repair in the central nervous system (Wang et al., 2006; Soundarapandian et al., 2011). Recently, ZNF488 has been proved to be an oncogene that promotes cell proliferation, epithelial mesenchymal transformation and tumorigenesis of nasopharyngeal carcinoma (Zong et al., 2016, 2019). Although the carcinogenic function of ZNF488 has been reported, its specific role in the development of cervical cancer is almost unknown. Therefore, the aim of this study was to evaluate the expression and participation of ZNF488 in CC and to explore its potential mechanism in carcinogenesis.

## Materials and methods

### *Data acquisition of database*

UALCAN is designed to provide the public with easily accessible cancer-OMICS data (TCGA and MET500). The expression of ZNF488 and correlation with the clinicopathological characteristics of CC were analyzed using UALCAN (http://ualcan.path.uab.edu) following the method described previously (Chandrashekar et al., 2017).

### *Tissue specimens*

55 CC tissues and paired adjacent normal tissues were collected from patients in Affiliated People's Hospital of Ningbo University. The inclusion criteria of the patients were as follows: i) Females diagnosed with CC using the International Federation of Gynecology and Obstetrics (FIGO, 2018) system; and ii) underwent biopsy or trachelectomy surgery. The exclusion criteria of the patients were as follows: i) Diagnosed with other tumors; ii) underwent radiotherapy or chemotherapy or any other treatment prior to surgery; and iii) CC recurrence. The study was conducted with the approval of the Ethics Committee of Affiliated People's Hospital of Ningbo University (The approval number: NBOG-2010A092M) and was based on all relevant principles of the Declaration of Helsinki. All patients gave written informed consent before participation in this study.

### *Cell lines*

Normal human cervical cell line (H8) and CC cell lines (SiHa, HeLa, C33a, HT-3 and Caski) were obtained from Chinese Academy of Sciences (Shanghai, China). All cell lines were cultured in Dulbecco's modified Eagle's medium (DMEM; Hycolne, South Logan, UT, USA) supplemented with 10% fetal bovine serum (FBS; Hycolne) and 1% penicillin-streptomycin (Hyclone). Cells were routinely placed in a humidified incubator under a condition of 5% $CO_2$ at 37°C.

### *Cell transfection*

For overexpression of ZNF488, cDNA was amplified and cloned into the pcDNA3.1 vector to generate pc-DNA3.1-ZNF488 vector (ZNF488), and the empty pc-DNA3.1 plasmid was used as a blank control (Vector). siRNAs interfering with ZNF488 (i.e. sh-ZNF488-1, 5′-GCGCCTTTAGCAAACCAAC-3′; sh-ZNF488-2, 5′-GCAAAGTGCAACCTGTCCT-3′) were designed and synthesized by RiboBio (Guangzhou, China). Transfection procedure was conducted using Lipofectamine 2000 (Thermo, Waltham, MA, USA).

### *Quantitative real-time polymerase chain reaction (qRT-PCR)*

Total RNA was isolated using the TRIzol Reagent (Invitrogen, Carlsbad, CA, USA) according to the manufacturer's instructions, and reversely transcribed into cDNAs using the PrimeScript RT Reagent Kit (Takara, Dalian, China). RT-qPCR was performed with SYBR Green Master Mix kit (Takara) on the Applied Biosystems 7500 Real-time RT-PCR system (Applied Biosystems, Carlsbad, CA, USA). GAPDH was used as the normalization control. The relative expression levels were calculated by the $2^{-\Delta\Delta CT}$ method. The PCR primer sequences are listed below: ZNF488, forward, 5'-CTTT CGCCTAACGTCCGA-3'; reverse,5'-GCTGTGAGAAG TCATGTGCC-3'; GAPDH, forward, 5'-CTCCTCCTGT TCGACAGTCAGC-3''; reverse, 5 '-CCCAATACGAC CAAATCCGTT-3'.

### *Cell counting kit-8 (CCK-8) assay*

CCK-8 (Beyotime, Shanghai, China) assay was employed to detect cell proliferation as instructed. Briefly, approximately $2\times10^3$ cells per well were plated into a 96-well plate. 10 μL CCK-8 solution was thereafter put into each well at 24, 48, 72, 96h after transfection and incubated for 4 hours at 37°C. The absorbances at 450 nm wavelength were examined using a microplate reader (Bio-Rad, Hercules, CA, USA).

### *Colony Formation Assay*

500 cells per well were placed in 6-well plates and the culture medium was replaced every 3 days. On day 14, colonies were fixed with 4% paraformaldehyde for 10 minutes and stained with 0.1% crystal violet for 15 minutes. The colonies were imaged and counted.

### *Flow cytometry analysis*

Flow cytometry was used to analyze the cell cycle progression of CC cells. In brief, $1\times10^5$ cells were seeded into 6-well plates and incubated for 48 hours. The cells were digested with trypsin, resuspended in

phosphate-buffered saline (PBS) and collected in centrifuge tubes. Then the cells were fixed with 70% ice-cold ethanol overnight at 4°C. After that, the cells were washed twice with PBS to remove ethanol and stained with 5 μL propidium iodide (PI, Beyotime) for 30 min at room temperature. Finally, cell cycle was evaluated using a FACSCalibur flow cytometer (BD Biosciences, San Jose, CA, USA).

### *In vivo tumorigenicity and lung metastasis*

BALB/c nude mice (aged 6 weeks, n=6 in each group) were used to establish a xenograft model. Briefly, $1\times10^6$ SiHa cells transfected with sh-NC or sh-ZNF488 were subcutaneously injected into the right side of nude mice. Tumor volumes were measured every 7 days. After 4 weeks, the mice were killed and tumor weights were analyzed. The tumor tissues were taken for immunohistochemistry (IHC) staining. Additionally, $1\times10^6$ SiHa cells transfected with sh-NC or sh-ZNF488 cells were tail vein injected into nude mice (4 mice per group), respectively. After 8 weeks, the lung tissues were surgically dissected and lung metastatic nodules were counted in each group. The animal study was permitted by the Institutional Animal Care and Use Committee of Affiliated People's Hospital of Ningbo University (NO. 2010AM312K).

Immunohistochemistry (IHC) staining. The mice tumor tissues were prepared and sliced into 4-μm-thick sections, then the sections were deparaffinized and rehydrated gradually. After that the sections were incubated with primary antibodies against ZNF488 (1:200, ab236581, Abcam, USA) and Ki-67 (1:800, ab245113, Abcam) overnight at 4°C. After washing the samples with PBS, the sections were incubated with horseradish peroxidase (HRP)-conjugated secondary antibody (HRP-conjugated goat anti-rabbit IgG,1:1000, ab6721, Abcam) for 1 hour at room temperature. Subsequently, the signal was amplified and visualized with 3′-diaminobenzidine (DAB) chromogens, and then counterstained with hematoxylin.

### *Transwell assay*

For migration assay, $1\times10^4$ cells suspended in 200 μL serum-free DMEM were seeded in the upper chamber (8 μm pore size, Corning, New York, USA) of an insert, while 500 μL DMEM with 10% FBS was added into the lower chamber. For the invasion assay, the upper chamber was pre-coated with 50 μL Matrigel (BD Biosciences, Franklin Lakes, NJ, USA) and incubated at 37°C for 30 min to solidify. After incubation for 24 hours, the cells remaining on the upper membrane were gently wiped with a cotton swab. Thereafter, the cells on the lower chamber were fixed with methanol and stained with 0.1% crystal violet solution (Beyotime) for 15 min at room temperature. Subsequently, the cells of five randomly selected fields were counted and photographed under an inverted microscope (Olympus, Tokyo, Japan).

### *Western blot*

The total proteins were extracted using radioimmunoprecipitation assay (RIPA) lysis buffer (Sigma, Aldrich, St. Louis, MO, USA) containing 10% phenylmethylsulfonyl fluoride (PMSF; Beyotime) and the protein concentration was quantified by Bicinchoninic Acid (BCA) Protein Assay Kit (Beyotime). The protein was separated with 10% denaturing sodium dodecyl sulfate-polyacrylamide gels electrophoresis (SDS-PAGE), and transferred onto polyvinylidene difluoride (PVDF) membranes (Millipore, Billerica, MA, USA). After blocking with 5% skim milk at room temperature for 1h, the membranes were incubated with the indicated primary antibodies at 4°C overnight and then incubated with HRP-conjugated secondary antibodies (Abcam) for 1h at room temperature. Finally, the blots were detected by enhanced chemiluminescence (Thermo Scientific, USA) according to the manufacturer's protocol. GAPDH was used as an internal control. The primary antibodies are as followed: ZNF488 (1:500, ab236581, Abcam), E-cadherin (1:50, ab1416, Abcam), N-cadherin (1:1000, ab18203, Abcam), MEK1/2 (1:20000, ab178876, Abcam), p-MEK1/2 (1:1000, ab194754, Abcam), ERK1/2 (1:10000, ab184699, Abcam), p-ERK1/2 (1:1000, ab201015, Abcam), cyclin D1 (1:200, ab16663, Abcam), CDK4 (ab137675, 1:500, Abcam), CDK6 (1:50000, ab124821, Abcam), GAPDH (ab8245, 1:500, Abcam).

### *Statistical analysis*

Statistical analysis was performed using SPSS 20.0 software (SPSS, Inc., Chicago, IL, USA) and GraphPad Prism 7.0 software (GraphPad Software, Inc., Chicago, USA). All experiments were performed in triplicate and the data were expressed as mean ± standard deviation (SD). The $\chi2$ test was applied to evaluate the association between the expression level of ZNF488 and clinical characteristics. Student's t-tests and one-way ANOVA with a Tukey post hoc test were used for estimating differences between two and among multiple groups. $P<0.05$ was defined as statistically significant.

## Results

### *ZNF488 is up-regulated in CC tissues and human CC cells*

First of all, the bioinformatics data analysis of The Cancer Genome Atlas (TCGA) dataset retrieved from UALCAN database (http://ualcan.path.uab.edu/analysis.html) revealed that ZNF488 expression was increased in CC tissues compared with the normal tissues and was associated with clinical stage and lymph node metastasis (Fig. 1A-C), suggesting that ZNF488 may be involved in the development of CC.

Consistently, the qRT-PCR and western blot results also confirmed the high expression of ZNF488 in 55 paired CC tissues compared with adjacent normal tissues (Fig. 1D-E). Next, we collected clinical information from these CC cases to evaluate the relationship between ZNF488 levels and clinicopathological features of these patients (Table 1). We identified that ZNF488 expression was significantly correlated with tumor size ($P$=0.010), FIGO stage ($P$=0.005), and lymph node metastasis ($P$=0.005). However, there was no obvious association in other clinical parameters, including age, degree of tumor differentiation, histological characteristics and HPV infection. Similarly, the qRT-PCR and western blot results (Fig. 1F-G) revealed that ZNF488 expression was also obviously elevated in CC cell lines (SiHa, HeLa, C33a, HT-3 and Caski) compared to normal Cervical Cells (H8). Taken together, these findings implied that ZNF488 may play an essential role in CC development and progression.

### *ZNF488 accelerates CC cell proliferation*

Next, to identify the biological function of ZNF488 in CC cells, the knockdown or overexpression efficiency of ZNF488 in SiHa and Caski cells was examined and is shown in Figure 2A-B. Due to the higher gene silencing efficiency of sh-ZNF488-1 in SiHa cells, we chose sh-ZNF488-1 (labeled as sh-ZNF488) for the subsequent functional experiments. Functionally, CCK-8 and colony formation assays demonstrated that ZNF488 reduction

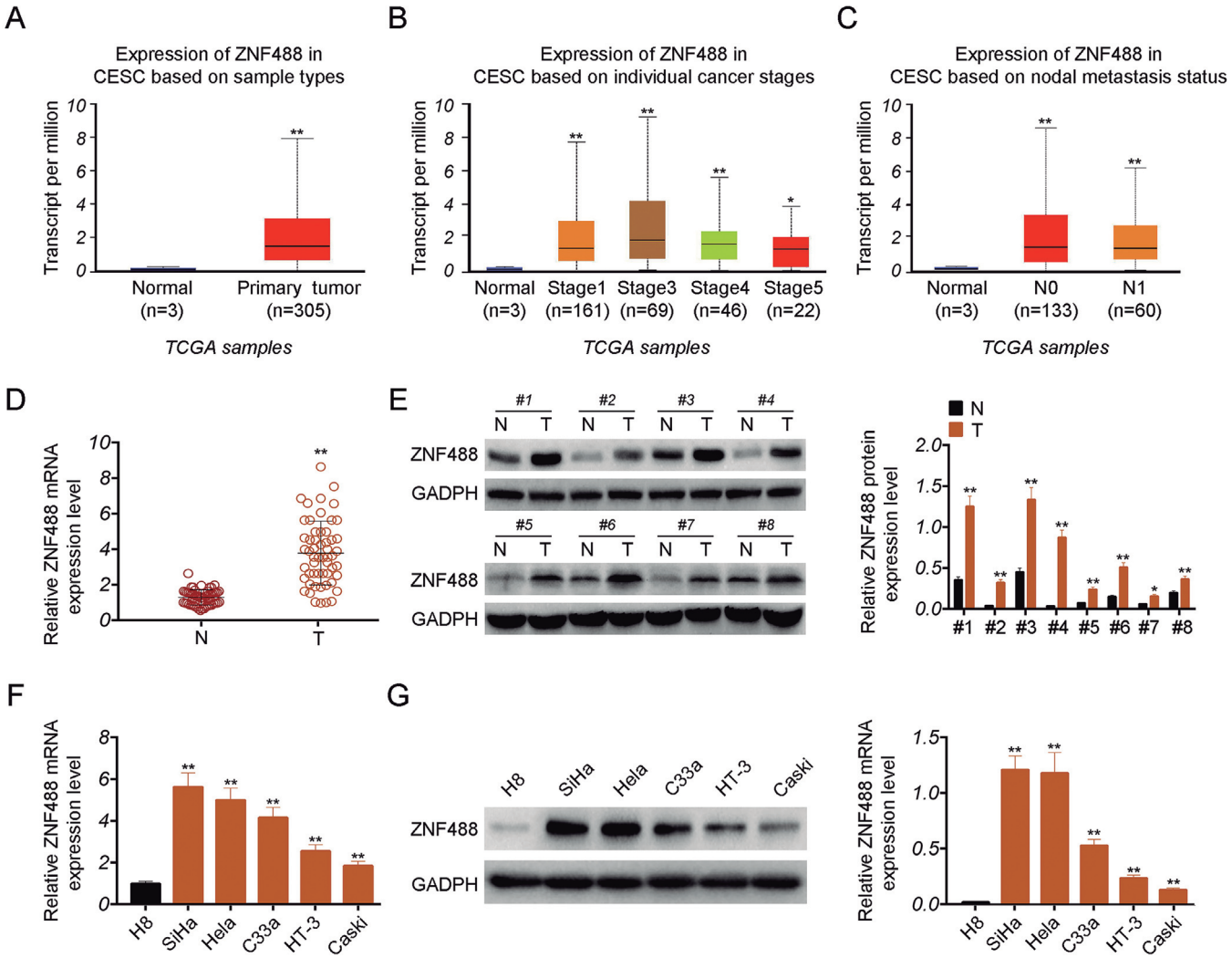


**Fig. 1.** ZNF488 is up-regulated in CC tissues and cells. **A.** UALCAN analysis of ZNF488 expression in The Cancer Genome Atlas (TCGA) database. **B.** UALCAN analysis of ZNF488 expression with different clinical stages. **C.** UALCAN analysis of ZNF488 expression with lymph node metastasis. **D.** The mRNA expression of ZNF488 in 55 CC tissues and the adjacent normal tissues were determined by qRT-PCR assay. **E.** The protein level of ZNF488 in CC tissues and the adjacent normal tissues was detected by western blot assay. **F.** The mRNA expression of ZNF488 in human CC cell lines (SiHa, HeLa, C33a, HT-3 and Caski) and normal cervical cells (H8) was determined by qRT-PCR assay. **G.** The protein level of ZNF488 in human CC cell lines (SiHa, HeLa, C33a, HT-3 and Caski) and normal cervical cells (H8) was detected by western blot assay. Data are shown as mean ± SD; $*P< 0.05$ and $**P<0.01$.

**Table1.** Correlation between the expression of ZNF488 and clinicopathological characteristics of patients with CC.

| Characteristics | Number of patients | ZNF488 Low expression (≤median) | ZNF488 High expression (>median) | *P* value |
|---|---|---|---|---|
| Number | 55 | 28 | 27 | |
| Ages(years) | | | | 0.549 |
| <45 | 25 | 13 | 12 | |
| ≥45 | 30 | 15 | 15 | |
| Tumor size (cm) | | | | 0.010* |
| <4 | 26 | 18 | 8 | |
| ≥4 | 29 | 10 | 19 | |
| Histology | | | | 0.454 |
| Squamous | 32 | 17 | 15 | |
| Adenocarcinoma | 23 | 11 | 12 | |
| FIGO stage | | | | 0.005** |
| Ib-IIa | 25 | 20 | 9 | |
| IIb-IIIa | 30 | 8 | 18 | |
| Differentiation | | | | 0.248 |
| Well/Moderate | 26 | 15 | 11 | |
| Poor | 29 | 13 | 16 | |
| Lymph node metastasis | | | | 0.005** |
| Negative | 25 | 18 | 7 | |
| Positive | 30 | 10 | 20 | |
| HPV infection | | | | 0.591 |
| Positive | 14 | 7 | 7 | |
| Negative | 41 | 21 | 20 | |

*$P$<0.05 and **$P$<0.01.

dramatically hindered the proliferation of SiHa cells whereas ZNF488 overexpression markedly increased the proliferation of Caski cells (Fig. 2C,D). According to the results of flow cytometric analysis, the deletion of ZNF488 induced G1 phase arrest in SiHa cells, while the upregulation of ZNF488 resulted in the decrease of G1 phase cells and the increase of S phase cells in Caski cells (Fig. 2E). These data suggested that ZNF488 contributed to cell proliferation of CC cells *in vitro*.

### *Knockdown of ZNF488 inhibits CC tumorigenesis in vivo*

*In vivo* xenograft mice models were constructed to further evaluate the effects of ZNF488 on the tumorigenicity of SiHa cells. SiHa cells stably transfected with sh-ZNF488 or sh-NC were subcutaneously injected into the Balb/c nude mice, the tumor volume was measured every 7 days from the first day of injection until 28th. The Representative image displayed that the tumors from sh-ZNF488 group were smaller than those from sh-NC group (Fig. 3A). Growth curve of tumor indicated that ZNF488 reduction significantly slowed the CC tumor growth (Fig. 3B). Consistently, the weight of tumor from sh-ZNF488 group was significantly reduced in contrast to the tumors form sh-NC group (Fig. 3C). Moreover, the results of IHC staining showed that knockdown of ZNF488 significantly downregulated expression of ZNF488 and

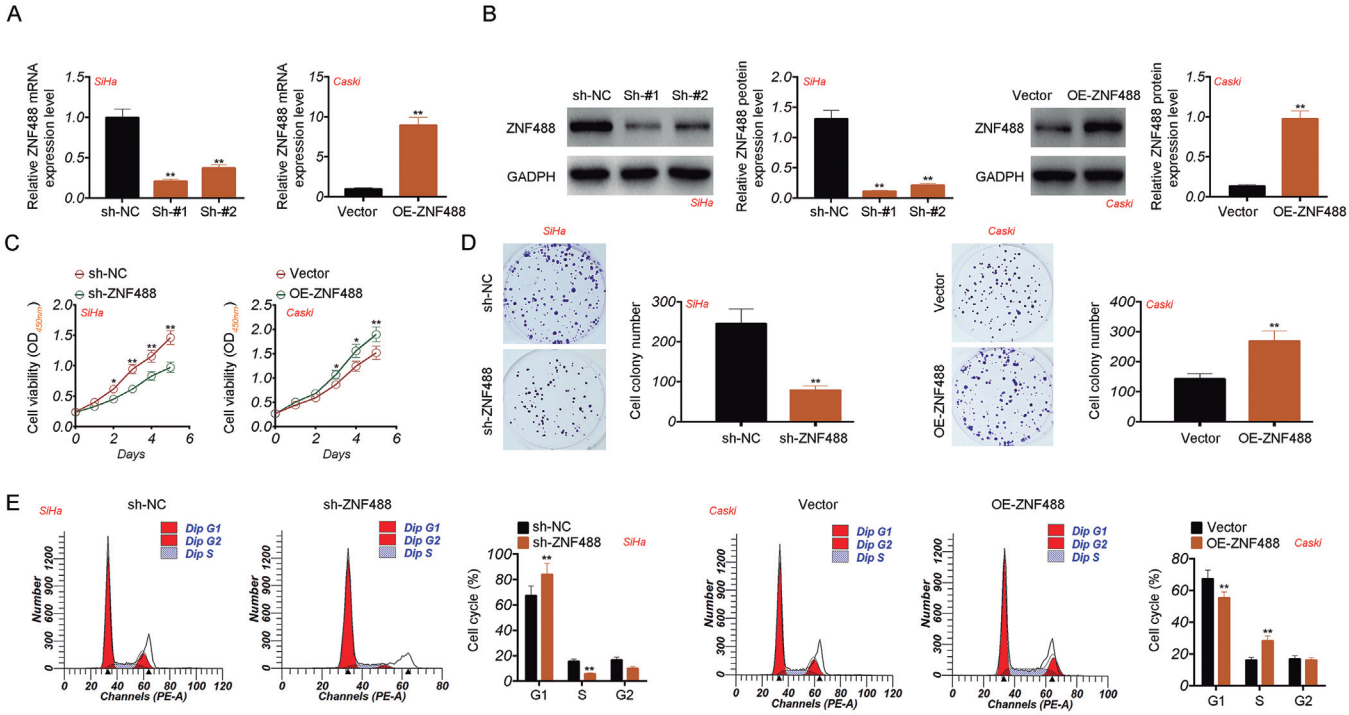


**Fig. 2.** ZNF488 accelerates CC cell proliferation. **A.** The mRNA expression of ZNF488 in SiHa and Caski cells was measured by qRT-PCR assay. **B.** The protein level of ZNF488 in SiHa and Caski cells was determined by western blot assay. **C.** CCK-8 assay was used to determine the cell viabilities of SiHa and Caski cells. **D.** Colony formation assay was used to detect the number of cell clones in SiHa and Caski cells. **E.** Flow cytometry assay was used to detect the distribution of cell cycle in SiHa and Caski cells. Data are shown as mean ± SD; *$P$<0.05 and **$P$<0.01.

Ki-67 in xenograft tumors (Fig. 3D). Collectively, the in vivo xenograft experiment demonstrated that knockdown of ZNF488 inhibited the growth of CC cells *in vivo*.

### *ZNF488 enhances CC cell metastasis capabilities*

We further assessed the effects of ZNF488 on the migratory and invasive capacities of CC cells *in vitro*. The results of migration and invasion transwell assays showed that knockdown of ZNF488 obviously attenuated cell migration and invasion in SiHa cells, while overexpression of ZNF488 increased cell migration and invasion in Caski cells (Fig. 4A-B). Further western blot analysis illustrated that knockdown of ZNF488 obviously increased the E-cadherin and decreased the N-cadherin expression in SiHa cells, whereas overexpression of ZNF488 exhibited an opposite result in Caski cells (Fig. 4C). To investigate if depletion of ZNF488 inhibits tumor metastasis in vivo, SiHa cells transfected with sh-ZNF488 or sh-NC were injected into the tail vein of nude mice. Deletion of ZNF488 resulted in a reduced number of metastatic nodules compared with the sh-NC group (Fig. 4D). In addition, HE staining of lung tissues also confirmed a significantly reduced number of metastatic nodules in the sh-ZNF488 group (Fig. 4E). Consistent with *in vitro* experiments, the down-regulation of ZNF488 increased the expression of E-cadherin and reduced the expression of N-cadherin (Fig. 4F). These *in vitro* and *in vivo* investigations revealed that ZNF488 promoted the CC metastasis process.

### *ZNF488 correlates with the MEK/ERK pathway*

The MEK/ERK signaling pathway is usually abnormally activated and plays a redundant role in the regulation of basic biological processes in various cancers, including cervical cancer (Manzo-Merino et al., 2014). To investigate the pathway by which ZNF488 is involved, we investigated the activation of MEK/ERK in SiHa and Caski cells. Western blot analysis (Fig. 5A-B) showed that knockdown of ZNF488 significantly downregulated the levels of p-MEK and p-ERK in SiHa cells, while overexpression of ZNF488 led to the opposite results. To confirm whether MEK/ERK is involved in the occurrence of cervical cancer mediated by ZNF488, the cells were cultured with 50μmol/L PD98059 (ERK inhibitor). Treatment with PD98059 reduced p-MEK and p-ERK expressions in Caski cells and reversed the activation of MEK/ERK pathway triggered by ZNF488 (Fig. 5B). Furthermore, inhibition of ERK by PD98059 was able to counteract the effects of overexpression of ZNF488 on the proliferation, migration and invasion related proteins of Caski cells (Fig. 5B). These results suggest that the MEK/ERK pathway is involved in the promotion of ZNF488 in CC progression.

## Discussion

The KRAB zinc finger encoded genes are the largest family of transcription/transcriptional regulators in mammals and bind to promoters of target genes to inhibit or activate their expression, thereby inhibiting or

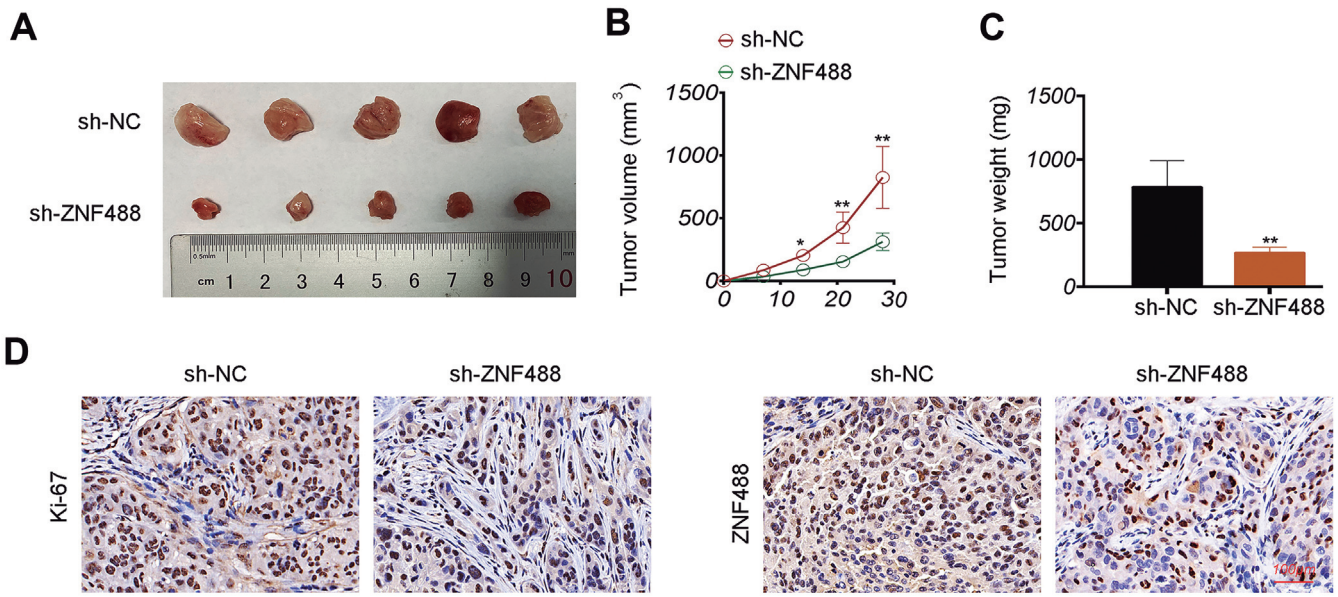


**Fig. 3.** Knockdown of ZNF488 inhibits CC tumorigenesis *in vivo*. **A.** Photographs of tumors excised from mice injected with SiHa cells transfected with sh-NC or sh-ZNF488. **B.** Tumor growth curves of mice injected with SiHa cells. **C.** Tumor weight of mice injected with SiHa cells. **D.** The levels of ZNF488 and Ki-67 in tumors from mice injected with SiHa cells were evaluated by IHC staining. Scale bar: 100 μm, magnification, 200×. Data are shown as mean ± SD; **P*<0.05 and ***P*<0.01.

promoting tumor progression (Urrutia, 2003; Lupo et al., 2013). Previous studies have shown that ZNF488 is a major up-regulated gene in nasopharyngeal carcinoma tissues and is associated with locoregional failure and distal metastasis. Patients with high expression of ZNF488 have poorer overall survival and progression-free survival time. In addition, high expression of ZNF488 was also found in 12 nasopharyngeal carcinoma cells (Zong et al., 2016, 2019). Similarly, Rajput et al. identified the differentially expressed genes (DEGs) and enrichment pathways involved in CC by studying gene expression Omnibus (GEO) microarray data (GSE44001) from 300 CC patients, of which ZNF488 was one of the DEGs highly expressed in cervical cancer samples (Rajput et al., 2020). Further, by analyzing the UALCAN database, we found that the expression of ZNF488 was also significantly increased in CC tissues compared with normal tissues, and was correlated with clinical staging and lymph node metastasis. In addition, we also confirmed that the expression level of ZNF488 was significantly up-regulated in the CC samples collected, and that the expression level of ZNF488 was increased in all the five CC cell lines. Therefore, ZNF488 may play an important role in the development of CC.

ZNF488 has been shown to be an oncogene that promotes invasion and tumogenesis in nasopharyngeal carcinoma by activating the Wnt/β-catenin pathway to induce EMT (Zong et al., 2016). It was found that ZNF488 can be used as an independent prognostic indicator of nasopharyngeal carcinoma and promote the proliferation and cycle progression of nasopharyngeal carcinoma cells through the collagen IV/FAK/Akt /Cyclin D1 pathway (Zong et al., 2019). Qiu et al. found that ZNF488 implicated invasion and migration of pancreatic cancer cells through the Akt/mTOR pathway (Qiu et al., 2022). In this study, we found for the first time that ZNF488 can promote the proliferation, migration and invasion of cervical cancer cells *in vitro*, and induce cell cycle progression. In addition, this study is the first to investigate the effects of ZNF488 on the promotion of xenograft tumor growth and lung metastasis.

ERK1/2 is considered to be typical mitogen-activated protein kinases (MAPKs) involved in signal transduction

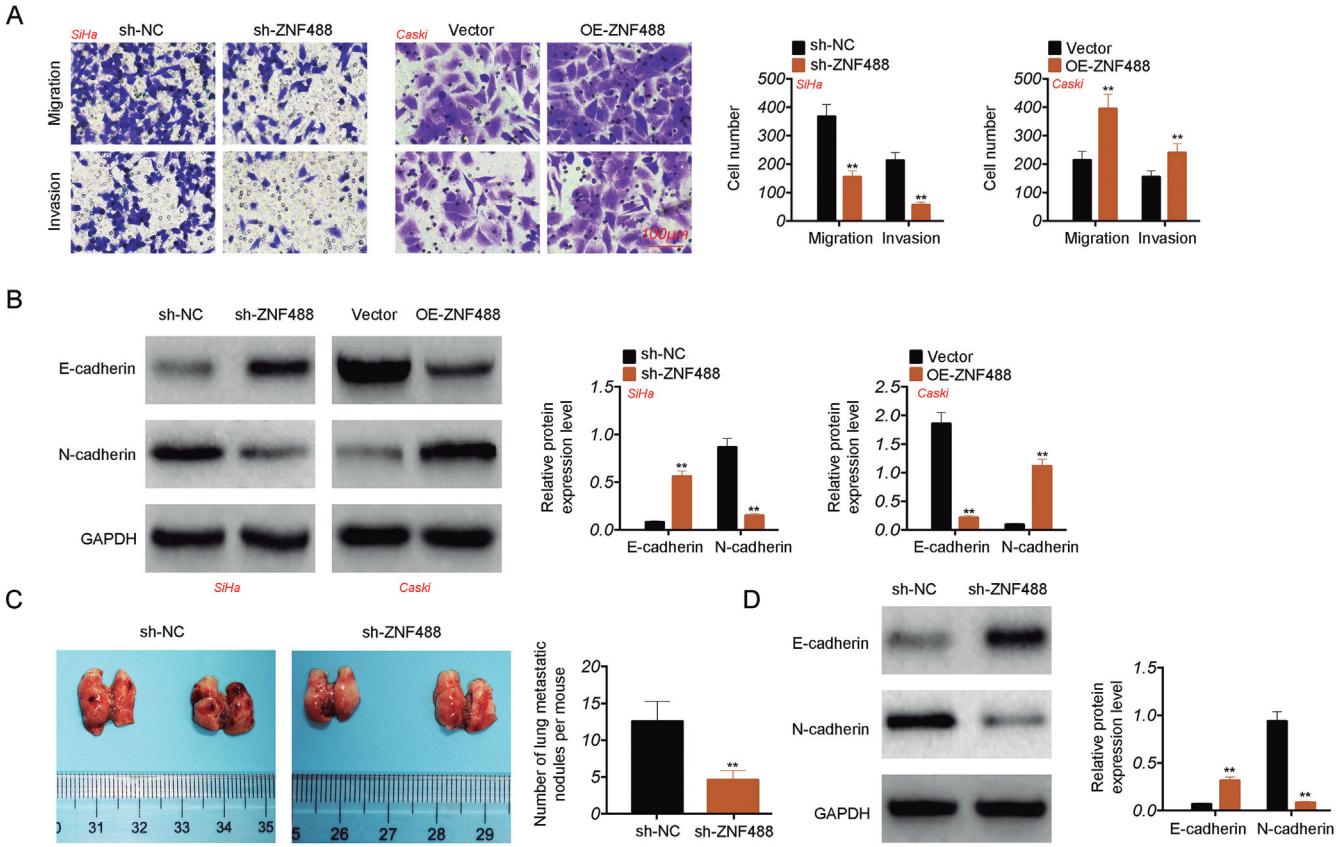


**Fig. 4.** ZNF488 enhances CC cells metastasis capabilities. **A.** Transwell assay was used to detect the migration and invasion capabilities of SiHa and Caski cells (Scale bar: 100 μm, magnification, 200×). **B.** The levels of E-cadherin and N-cadherin in SiHa and Caski cells were measured by western blot analysis. **C.** Representative images of lung colonization after injection of SiHa cells into the tail veins of mice. **D.** The levels of E-cadherin and N-cadherin in lung tissues were measured by western blot analysis. Data are shown as mean ± SD; ***P*<0.01.

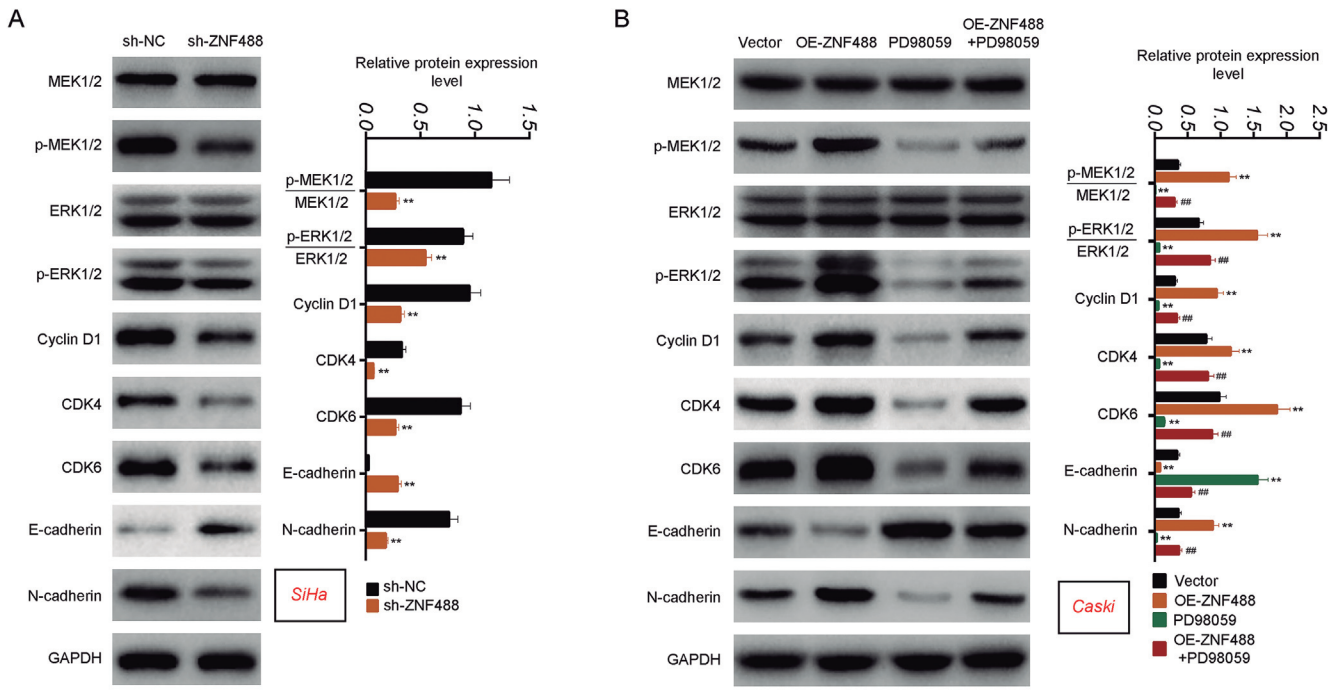


**Fig. 5.** ZNF488 correlates with the MEK/ERK pathway. **A.** The levels of MEK1/2, p-MEK1/2, ERK1/2, p-ERK1/2, Cyclin D1, CDK4, CDK6, E-cadherin, N-cadherin in SiHa cells were evaluated by western blot assay. **B.** The levels of MEK1/2, p-MEK1/2, ERK1/2, p-ERK1/2, Cyclin D1, CDK4, CDK6, E-cadherin, N-cadherin in Caski cells were evaluated by western blot assay. Western blot analysis of the indicated proteins after treatment with 10 μM PD98059 for 72 h. Data are shown as mean ± SD; compared to sh-NC/Vector group, $^{**}P<0.01$, compared to PD98059 group, $^{\#\#}P<0.01$.

and transcriptional regulation (Guo et al., 2020). The nuclear translocation of ERK1/2 in cell biology is dependent on its phosphorylation form (p-ERK1/2), and ERK1/2 is phosphorylated by its upstream factor p-MEK1/2 (Wan et al., 2004; Ritt et al., 2016). Many zinc finger proteins have been reported to affect cell biological functions through the ERK/MEK pathway, such as ZNF540, ZNF545, ZNF580, ZNF251 and ZNF278, etc (Xiang et al., 2006, 2017; Luo et al., 2014; Tian et al., 2017; Zhong et al., 2020). By phosphorylation of ERK Thr202 and TYR204, ZNF251 can activate ERK signal to promote the proliferation and tumor formation of lung cancer cells (Zhong et al., 2020). ZNF545 can inhibit the proliferation and migration of colorectal cancer cells by regulating the ERK signaling pathway (Xiang et al., 2017). However, the mechanism by which ZNF488 plays a similar role in ERK/MEK pathway in CC has not been publicly documented until we conducted this study. In this study, we found that ZNF488 promoted the activation of ERK/MEK signaling pathway in CC cells, and inhibited ERK/MEK signaling with ERK inhibitor PD98059, reversing the effects of overexpression of ZNF488 on proliferation, migration and invasion of CC cells. These data suggest that the role of ZNF488 in promoting CC progression may be through the MEK/ERK signaling pathway.

In conclusion, our results suggest that ZNF488 is involved in the occurrence and development of CC through MEK/ERK pathway, indicating that ZNF488 may provide a new feasible molecular target for clinical studies of CC.

*Acknowledgements.* Thank you for the support of Ethics Committee of Affiliated People's Hospital of Ningbo University. Thanks to all patients who participated in the study for their understanding and cooperation.

*Funding.* No funding was received.

*Competing interests.* The authors state that there are no conflicts of interest to disclose.

*Availability of data and materials.* All data generated or analyzed during this study are included in this published article.

*Authors' contributions.* KNW designed the study, supervised the data collection, analyzed the data, LL interpreted the data and prepare the manuscript for publication, and HPZ supervised the data collection, analyzed the data and reviewed the draft of the manuscript.

All authors have read and approved the manuscript.

*Patient consent for publication.* Patients signed informed consent for potential publication of the present paper.

*Ethics approval and consent to participate.* All experiments in this study were approved by the Animal Care and Use Committee of Affiliated People's Hospital of Ningbo University (NO. 2010AM312K) and performed in accordance with the Guide for the Care and Use of Laboratory Animals.

*Informed consent.* Written informed consent was obtained from a legally authorized representative(s) for anonymized patient information to be published in this article.

## References

Canfell K. (2019). Towards the global elimination of cervical cancer. Papillomavirus Res. 8, 100170.

Cassandri M., Smirnov A., Novelli F., Pitolli C., Agostini M., Malewicz M. and Raschellà G. (2017). Zinc finger proteins in health and disease. Cell Death Dis. 3, 17071.

Chandrashekar D.S., Bashel B., Balasubramanya S.A.H., Creighton C.J., Ponce Rodriguez I., Chakravarthi B.V.S.K. and Varambally S. (2017). UALCAN: A portal for facilitating tumor subgroup gene expression and survival analyses. Neoplasia 19, 649658.

Crosbie E.J., Einstein M.H., Franceschi S. and Kitchener H.C. (2013). Human papillomavirus and cervical cancer. Lancet 382, 889899.

De Sanjose S., Quint W.G., Alemany L., Geraets D.T., Klaustermeier J.E., Lloveras, B. and Bosch F.X. (2010). Human papillomavirus genotype attribution in invasive cervical cancer: a retrospective crosssectional worldwide study. Lancet Oncol. 11, 10481056.

Denny L. (2012). Cervical cancer: prevention and treatment. Discov. Med. 14, 125131.

Guo Y.J., Pan W.W., Liu S.B., Shen Z.F., Xu Y. and Hu L.L. (2020). ERK/MAPK signalling pathway and tumorigenesis (Review). Exp. Ther. Med. 19, 19972007.

Hashemipour M., Boroumand H., Mollazadeh S., Tajiknia V., Nourollahzadeh Z., Rohani Borj M. and Mirzaei H. (2021). Exosomal microRNAs and exosomal long noncoding RNAs in gynecologic cancers. Gynecol. Oncol. 161, 314327.

Hoovers J.M.N., Mannens M., John R., Bliek J., van Heyningen V., Porteous D.J. and Little P.F.R. (1992). High resolution localization of 69 potential human zinc finger protein genes: A number are clustered. Genomics 12, 254263.

Hu X., Schwarz J.K., Lewis J.S., Jr., Huettner P.C., Rader J.S., Deasy J.O. and Wang X. (2010). A microRNA expression signature for cervical cancer prognosis. Cancer Res. 70, 14411448.

Luo Y., Zhao Y., Li X., Zhao J. and Zhang W. (2014). ZNF580 mediates eNOS expression and endothelial cell migration/proliferation via the TGFβ1/ALK5/Smad2 pathway. Mol. Cell. Biochem. 393, 199207.

Lupo A., Cesaro E., Montano G., Zurlo D., Izzo P. and Costanzo P. (2013). KRAB zinc finger proteins: a repressor family displaying multiple biological functions. Curr. Genomics 14, 268278.

Manzo Merino J., Contreras Paredes A., Vázquez Ulloa E., Rocha Zavaleta L., Fuentes Gonzalez A.M. and Lizano M. (2014). The role of signaling pathways in cervical cancer and molecular therapeutic targets. Arch. Med. Res. 45, 525539.

Miller J., McLachlan A.D. and Klug A. (1985). Repetitive zinc binding domains in the protein transcription factor IIIA from Xenopus oocytes. EMBO J. 4, 16091614.

Nagaoka M. and Sugiura Y. (2000). Artificial zinc finger peptides: creation, DNA recognition and gene regulation. J. Norg. Biochem. 82, 5763.

Nahand J.S., Vandchali N.R., Darabi H., Doroudian M., Banafshe H.R., Moghoofei M. and Mirzaei H. (2020). Exosomal microRNAs: novel players in cervical cancer. Epigenomics. 12, 16511660.

Pal A. and Kundu R. (2020). Human papillomavirus E6 and E7: The cervical cancer hallmarks and targets for therapy. Front Microbiol.10, 3116.

Qiu H., Zhang L., Wang D., Zhang Y., Cai H., Miao H. and Chu F. (2022). ZNF488 promotes the Invasion and migration of pancreatic carcinoma cells through the Akt/mTOR pathway. Comput. Math. Method. Med. 2022, 4622877.

Rahimian N., Razavi Z.S., Aslanbeigi F., Mirkhabbaz A.M., Piroozmand H., Shahrzad M.K. and Mirzaei H. (2021). Noncoding RNAs related to angiogenesis in gynecological cancer. Gynecol. Oncol. 161, 896912.

Rajput M., Kumar M., Kumari M., Bhattacharjee A. and Awasthi A.A. (2020). Identification of key genes and construction of regulatory network for the progression of cervical cancer. Gene Rep. 21, 100965.

Razavi Z.S., Tajiknia V., Majidi S., Ghandali M., Mirzaei H.R., Rahimian N. and Mirzaei H. (2021). Gynecologic cancers and noncoding RNAs: Epigenetic regulators with emerging roles. Crit. Rev. Oncol. Hematol. 157, 103192.

Ritt D.A., AbreuBlanco M.T., Bindu L., Durrant D.E., Zhou M., Specht S.I. and Morrison D.K. (2016). Inhibition of Ras/Raf/MEK/ERK pathway signaling by a stress-induced phospho-regulatory circuit. Mol. Cell. 64, 875887.

Small Jr W., Bacon M.A., Bajaj A., Chuang L.T., Fisher B.J., Harkenrider M.M. and Gaffney D.K. (2017). Cervical cancer: A global health crisis. Cancer 123, 24042412.

Soundarapandian M.M., Selvaraj V., Lo U.G., Golub M.S., Feldman D.H., Pleasure D.E. and Deng W. (2011). Zfp488 promotes oligodendrocyte differentiation of neural progenitor cells in adult mice after demyelination. Sci. Rep. 1, 2.

Stevanović S., Draper L.M., Langhan M.M., Campbell T.E., Kwong M.L., Wunderlich J.R. and Hinrichs C.S. (2015). Complete regression of metastatic cervical cancer after treatment with human papillomavirustargeted tumorinfiltrating T cells. J. Clin. Oncol. 33, 15431550.

Tian X.Q., Guo F.F., Sun D.F., Wang Y.C., Yang L., Chen S.L. and Fang J.Y. (2017). Downregulation of ZNF278 arrests the cell cycle and decreases the proliferation of colorectal cancer cells via inhibition of the ERK/MAPK pathway. Oncol. Rep. 38, 36853692.

Urrutia R. (2003). KRAB-containing zinc-finger repressor proteins. Genome Biol. 4, 231.

Wan P.T.C., Garnett M.J., Roe S.M., Lee S., NiculescuDuvaz D., Good, V.M. and Marais R. (2004). Mechanism of activation of the RAF-ERK signaling pathway by oncogenic mutations of B-RAF. Cell 116, 855867.

Wang S.Z., Dulin J., Wu H., Hurlock E., Lee S.E., Jansson K. and Lu Q.R. (2006). An oligodendrocytespecific zinc finger transcription regulator cooperates with Olig2 to promote oligodendrocyte differentiation. Development 133, 33893398.

Xiang Z., Yuan W., Luo, N., Wang Y., Tan K., Deng Y. and Liu M. (2006). A novel human zinc finger protein ZNF540 interacts with MVP and inhibits transcriptional activities of the ERK signal pathway. Biochem. Bioph. Res. Commun. 347, 288296.

Xiang S., Xiang T., Xiao Q., Li Y., Shao B. and Luo T. (2017). Zinc finger protein 545 is inactivated due to promoter methylation and functions as a tumor suppressor through the Wnt/βcatenin, PI3K/AKT and MAPK/ERK signaling pathways in colorectal cancer. Int. J. Oncol. 51, 801811.

Zhong C., Chen C., Yao F. and Fang W. (2020). ZNF251 promotes the progression of lung cancer by activating ERK signaling. Cancer Sci. 111, 32363244.

Zong D., Jiang N., Xu J.H., Wang D.J., Zhu H.F., Wu L.R. and He X. (2019). ZNF488 is an independent prognostic indicator in nasopharyngeal carcinoma and promotes cell adhesion and proliferation via collagen IV/FAK/AKT/Cyclin D1 pathway. Cancer Manag. Res. 11, 58715882.

Zong D., Yin L., Zhong Q., Guo W.J., Xu J.H., Jiang N. and Zeng M.S. (2016). ZNF488 enhances the invasion and tumorigenesis in nasopharyngeal carcinoma via the Wnt signaling pathway involving epithelial mesenchymal transition. Cancer Res. Treat. 48, 334344.

Accepted December 2, 2022